

Global Conformation of Tau Protein Mapped by Raman Spectroscopy

Nalini Vijay Gorantla, Puneet Khandelwal, Pankaj Poddar,
and Subashchandra Chinnathambi

Abstract

Alzheimer's disease (AD) is one of the neurodegenerative disease characterized by progressive neuronal loss in the brain. Its two major hallmarks are extracellular senile plaques and intracellular neurofibrillary tangles (NFTs), formed by aggregation of amyloid β -42 ($A\beta$ -42) and Tau protein respectively. $A\beta$ -42 is a transmembrane protein, which is produced after the sequential action of β - and γ -secretases, thus obtained peptide is released extracellularly and gets deposited on the neuron forming senile plaques. NFTs are composed of microtubule-associated protein-Tau (MAPT). Tau protein's major function is to stabilize the microtubule that provides a track on which the cargo proteins are shuttled and the stabilized microtubule also maintains shape and integrity of the neuronal cell. Tau protein is subjected to various modifications such as phosphorylation, ubiquitination, glycation, acetylation, truncation, glycosylation, deamination, and oxidation; these modifications ultimately lead to its aggregation. Phosphorylation is the major modification and is extensively studied with respect to Tau protein. Tau protein, however, undergoes certain level of phosphorylation and dephosphorylation, which regulates its affinity for microtubule and ultimately leading to microtubule assembly and disassembly. Our main aim was to study the native state of longest isoform of Tau (hTau40WT-4R2N) and its shortest isoform, (hTau23WT-3R0N), at various temperatures such as 10, 25, and 37 °C. Raman spectroscopic results suggested that the proportion of random coils or unordered structure depends on the temperature of the protein environment. Upon increase in the temperature from 10 to 37 °C, the proportion of random coils or unordered structures increased in the case of hTau40WT. However, we did not find a significant effect of temperature on the structure of hTau23WT. This current approach enables one to analyze the global conformation of soluble Tau in solution.

Key words Tau protein, Tau conformation, Tau aggregation, Alzheimer disease, Sedimentation assay, Raman spectroscopy

1 Introduction

Tau belongs to a class of proteins called microtubule-associated proteins (MAPs) whose major function is to stabilize microtubules (MT) that serve as cytoskeleton. Microtubules are important for cell viability, cell polarity, and particularly for development of neurons. The main biological function of Tau is to stimulate

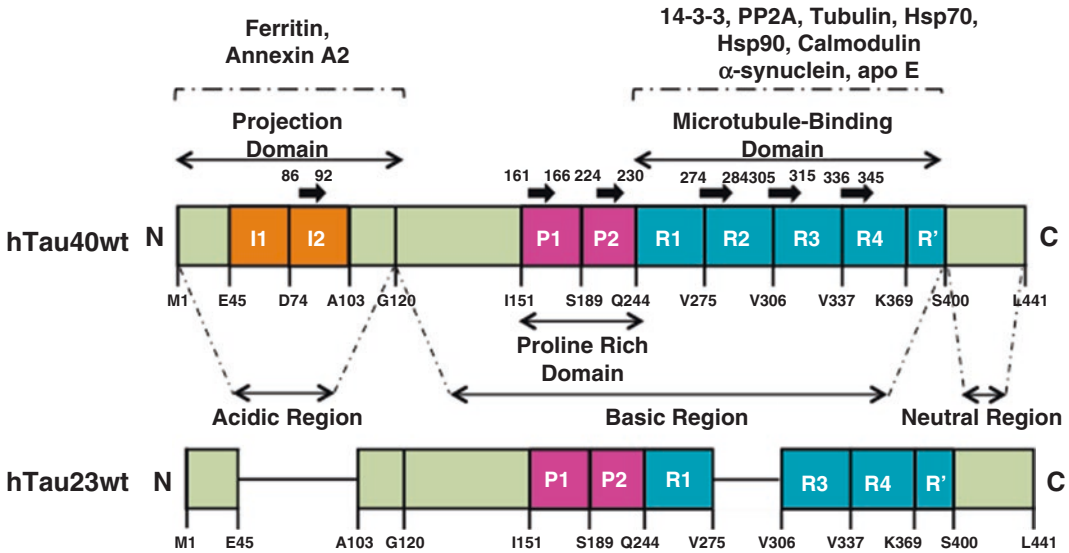


Fig. 1 Schematic presentation of Human Tau protein. Tau protein has an overall basic charge with N-terminal acidic region, basic repeat region and neutral C-terminal. Bar diagrams of hTau40WT and hTau23WT, the longest and the shortest isoform respectively are depicted. hTau40WT has 441 amino acids that include two inserts, I1 and I2, encoded by exon 2 and 3, located at the N-terminal end. This is followed by P1 and P2, the proline-rich regions. R1, R2, R3, and R4 are the four imperfect repeats present towards the C-terminal end. These repeats are binds to tubulin and also responsible for its assembly into microtubule. Many proteins interact with Tau in its N-terminal as well as in the repeat region. Tau protein is highly soluble with no secondary structures, but however it forms transient β -sheet, indicated by black arrows. hTau23WT is the shortest isoform that lacks I1, I2, and R2, which are encoded by exon 2, 3, and 10

microtubule assembly and to stabilize the structure of microtubules (Fig. 1). Tau is a phosphoprotein and its phosphorylation state is developmentally regulated [1–7]. Tau protein is one of the most soluble, natively unfolded, which does not adapt any secondary structure (Fig. 1). However, it forms transient α -helix or β -sheet structures on binding to its interacting partners. Tau protein in Alzheimer’s disease (AD) condition forms toxic β -rich aggregates, leading to neurodegeneration. Tau protein has been studied using different spectroscopic techniques in order to understand its structural conformations. The analysis of sedimentation assay and circular dichroism (CD) showed Tau to be a highly asymmetric molecule with very little secondary structure in solution [8–10]. The extensive investigation of Tau structure in solution using X-ray scattering and CD revealed that Tau behaves as a random Gaussian coil with persistence length of ~ 2 nm [11–15]. Intrinsic fluorescence analysis of tryptophan mutants of Tau confirmed that residues along the polypeptide chain were indeed completely solvent exposed, supporting the lack of structure [16]. All these observations clearly demonstrate that Tau in solution does not contain any secondary structure and can be regarded as ‘natively unfolded protein’ [11, 17–19]. In addition, nuclear magnetic resonance (NMR) was performed for Tau protein in its

longest as well as shortest isoform; Mandelkow [16, 20–25] and Lippens group in 2006 [26, 27] elucidated the use of NMR to study the residual structures not only in the soluble form but also in the aggregates of Tau protein. This revealed the highly dynamic property of Tau and also showed that transient long-range interactions are necessary for aggregate formation [16, 20–25]. Further efforts to visualize Tau in electron microscope suffered from its low contrast due to its low-*z* number as well as hydrophilic nature (carbon coated TEM grids being hydrophobic-resulting into poor coating) [28], but the glycerol-spray technique clearly revealed the structure of Tau to be an elongated and flexible rod, about 35 nm in length [29]. The global hairpin conformation of Tau protein was explained using fluorescence resonance energy transfer (FRET) technique and electron paramagnetic resonance (EPR) [16, 30–32]. EPR showed the importance of second and third repeat in the formation of protease resistant core region of aggregates [32]. Tau adopts a “paperclip” conformation, whereby the N- and C-terminal domains approach each other and also the repeat domain [30, 32]. Tau protein is subjected to various insults before aggregating and one such is hyperphosphorylation by many cellular kinases. There are many distinct sites of phosphorylation; these were answered using matrix-assisted laser desorption/ionization-Fourier transform ion cyclotron resonance-mass spectroscopy (MALDI-FTICR-MS) [33]. In addition, small-angle X-ray scattering (SAXS) and FRET were used to obtain insight into the structure of the Tau protein [16, 18, 30, 31, 34–37]. These methods revealed that 441-residue Tau is highly dynamic in solution with a distinct domain character and an intricate network of transient long-range contacts important for pathogenic aggregation [28, 37]. Several attempts were made to understand the structure of Tau in soluble as well as aggregated form, but still it remains partially unresolved. The plausible reason is that being natively unfolded, Tau protein may not have static structures (α -helix or β -sheet), but possibly it may adapt an ensemble of dynamically interchanging secondary structure conformations, which limits the application of standard structural biology tools for structural determination [38]. Raman spectroscopy has the potential to characterize the change in the conformational states induced by environmental changes.

Raman spectroscopy has been widely used to noninvasively investigate the changes in secondary structure at all stages of protein aggregation and amyloid fibril formation. Raman spectroscopy is an inelastic light scattering technique that scatters the monochromatic light on interacting with the sample (Fig. 2). The wavelength of the light emitted from the sample will be higher (Stokes scattering) or lower (anti-Stokes scattering) depending on the loss or gain of the energy by the light photon. Nevertheless, in Raman spectroscopy, Stokes scattering is considered in the spectrum due to its higher intensity. But only 1 in 10^7 photons exhibits Stokes scattering due to its feeble scattering cross-section, anti-stoke

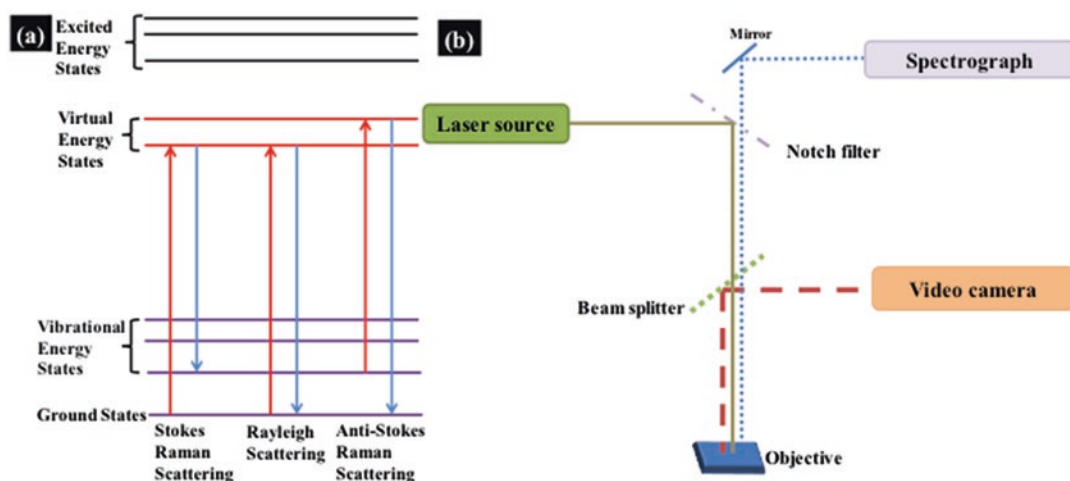


Fig. 2 (a) Principle of Raman effect and (b) instrumentation. When the sample is illuminated with a monochromatic laser beam (green color), the exchange of quantum vibrational energy occurs, which results in a change in the energy of scattered light. However, most of the scattered light has the same energy (elastic scattering) as the incident light and is referred to as Rayleigh scattering. Only a very small amount (1 in 10^7 photons) of scattered light (elastic scattering) can be of higher or lower vibrational energies depending on the vibrational state of the molecule and can be referred to as Stokes and anti-Stokes Raman scattering. The Raman shifted light (blue color) will filter from the notch filter and be detected by a CCD detector.

being still lesser and Rayleigh's scattering being more prominent. In order to increase the scattering cross-section, there are several enhancements in Raman spectroscopy, such as surface-enhanced Raman spectroscopy (SERS), tip-enhanced Raman spectroscopy (TERS), Raman optical activity (ROA), resonance Raman, coherent anti-Stokes Raman, and deep UV resonance Raman spectroscopy (DUVRR), etc. The β -sheet conformation of poly-(L-lysine) was studied using vibrational ROA and the structural transitions were also monitored against the function of time [39]. The Tau protein before forming stable aggregates goes through several intermediate structures, such as oligomers, protofilaments, and fibrils. Raman spectroscopy can be used to study these transitions in structure and trace their conformational path [40]. Raman is also coupled to techniques such as atomic force microscopy (AFM), scanning electron microscopy (SEM), and vibrational circular dichroism (VCD) to study the morphology of the amyloid fibrils [41–43]. Elucidation of the structural details of these aggregated proteins is challenging. The morphology of aggregates is different based on different interacting partners, such as metal ions [42] and lipids [44]. Similarly, the effect of temperature, pH, ionic strength, etc. on the protein can be studied using Raman spectroscopy [43]. Recently, Ramachandran et al., employed the UV resonance Raman spectroscopy to look at the signatures of changes in secondary structure and side-chain packing during fibril formation by the four repeat functional domain of Tau in the presence of the inducer heparin [45]. However, there is a lack of Raman study on

the natively unfolded Tau protein and its temperature dependence. In this chapter, hTau40WT and hTau23WT are studied in their native condition using a combination of sedimentation analysis and Raman spectroscopy as a function of temperature such as 10, 25, and 37 °C.

The Raman spectroscopic technique is established as a very useful probe to study the structure of natively unfolded proteins (one of the example is Tau protein) [46, 47]. In view of this fact, the Raman spectroscopic measurements were performed on hTau40WT and hTau23WT at three different temperatures such as 10, 25, and 37 °C (Fig. 3a) to analyze the effect of temperature on the secondary structural content of these proteins. Figure 3a shows the Raman spectra of hTau40WT and hTau23WT proteins and the Fig. 3b shows the enlarged area from 1600 to 1700 cm^{-1} , which compares the amide I band for all the cases. Amide I band is very important in assigning the peptide backbone conformation in protein structure [45]. Generally, the presence of an amide I band centered between 1650 and 1658 cm^{-1} shows the presence of a high α -helical content, the Raman band in the range 1660–1665 cm^{-1} shows high proportions of random coil, and the Raman band in the range 1665–1680 cm^{-1} indicated unordered structure, and β -sheet structures. It can be easily noticed from the Fig. 3b that the intensity of amide I band was more in the case of hTau40WT in comparison to hTau23WT. This observation supports the fact that hTau23WT is a shorter construct of hTau40WT. Raman spectra for hTau40WT at different temperatures show that the structure of the protein is dynamic in nature and can be changed upon change in the environment temperature. The amide I band of the hTau40WT was broad, which suggest the presence of various

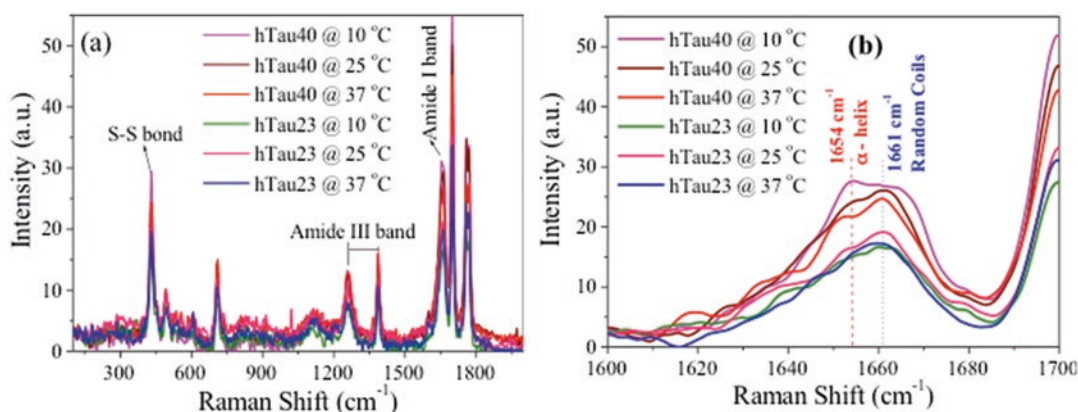


Fig. 3 Tau conformation mapped by Raman spectroscopy. Raman spectroscopy is established as a very useful technique to study the secondary structure of protein molecules, especially, natively unfolded proteins (such as Tau), which do not have the defined secondary structure in their native states. (a) Raman spectra of hTau40WT and hTau23WT proteins at various temperatures 10, 25, and 37 °C, and (b) respective enlarged view of amide I band

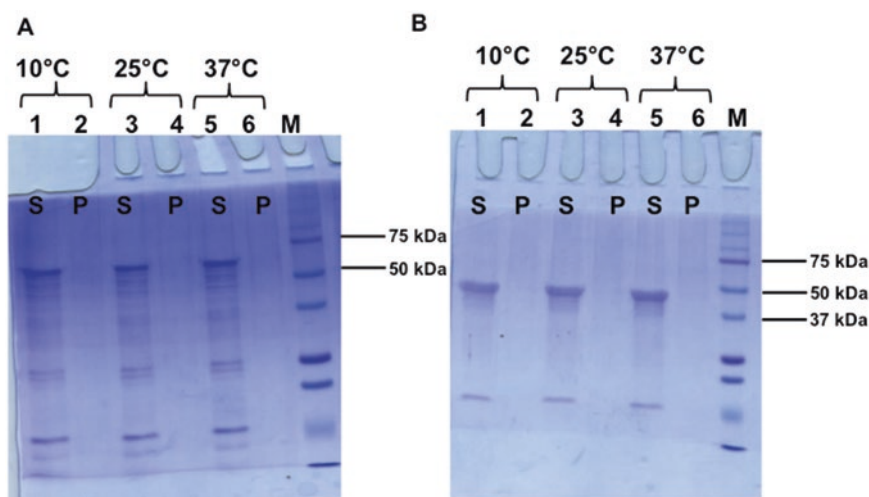


Fig. 4 Sedimentation assay of soluble hTau40WT (**a**) and hTau23WT (**b**) at different temperatures (10, 25, and 37 °C). Supernatant and pellet fractions obtained after sedimentation assay at different temperatures were run on 10 % SDS-polyacrylamide gel. Notation 1 and 2; 3 and 4; 5 and 6 denotes supernatant and pellet at 10, 25, and 37 °C, respectively on the SDS-PAGE. Soluble protein was found in supernatant fraction. These results clearly suggest that the structural changes solely come from temperature

secondary structures in the protein molecule, and can be considered as a doublet. The spectra recorded at 10 °C for hTau40WT shows the most prominent peak $\sim 1654\text{ cm}^{-1}$, and the less intense peak $\sim 1664\text{ cm}^{-1}$, related to a high proportion of α -helix and a small proportion of random coils as well as β -sheets. However, upon further increase in the temperature to 25 and 37 °C, leads to the clear shift of the most prominent peak to $\sim 1661\text{ cm}^{-1}$ which indicates the presence of a high proportion of random coils or unordered structures, apparently, with a small proportion of α -helix and β -sheets. However, the significant changes in the structure of hTau23WT, as a function of environmental temperature was not observed. The presence of amide I band $\sim 1661\text{ cm}^{-1}$ shows the presence of a high proportion of random coils or unordered structure at all the three temperatures (10, 25, and 37 °C).

2 Materials

1. Protein sample buffer (Raman spectroscopy): 50 mM phosphate buffer, pH 6.8.
2. BCA Protein Assay.
3. 5 μM BSA in 50 mM phosphate buffer, pH 6.8.
4. Microcentrifuge, such as Eppendorf 5418 R; rotor FA-45-18-11 (Eppendorf).
5. SDS Laemmli sample buffer 5X.

6. Coomassie Brilliant Blue R-250 staining solution: 45 % methanol, 10 % glacial acetic acid, 45 % water, 2.5 g/L Coomassie Brilliant Blue R-250; dissolve 2.5 g Coomassie Brilliant Blue R-250 in 450 mL methanol, mix 100 mL acetic acid to 450 mL water and add to the Coomassie dye solution, and filter.
7. HR-800 Raman spectrophotometer (Jobin Yvon-Horiba, France).

3 Methods

3.1 Protein Preparation

Expression of Tau isoforms (*see* Fig. 1) in *E. coli* and purification is described in Chapter 1 and in [48] (*see* Notes 1 and 2).

3.2 Tau Conformation Monitored by Sedimentation Assay

1. The protein concentrations are measured by using bicinchoninic acid (BCA) assay and concentrations of hTau40WT and hTau23WT are estimated as 26.3 and 18.5 mg/mL, respectively. Bovine serum albumin (BSA) is used as standard. The proteins are aliquoted and stored them in -80°C (*see* Note 1).
2. The protein aliquot at -80°C is allowed to thaw on ice and is centrifuged at 4°C and $20,800\times g$ for 1 h (*see* Notes 2 and 3).
3. 50 μL of 1 mg/mL protein dilutions of soluble Tau (hTau40WT and hTau23WT) are prepared and incubated at 10, 25, and 37°C for 30 min. After incubation samples are centrifuged at $20,800\times g$ for 30 min at 10, 25, and 37°C respectively (*see* Notes 4 and 5).
4. 50 μL supernatant is carefully transferred into other tube after centrifugation. The pellet is resuspended in 50 μL of Protein sample buffer (*see* Note 6).
5. SDS sample buffer is added to supernatant and pellet fraction and these are resolved by 10 % SDS-polyacrylamide gel electrophoresis (Fig. 4a, b).
6. The percentage of Tau isoforms (hTau40WT and hTau23WT) in the supernatants and pellets are quantified by densitometry of Coomassie Brilliant Blue R-250 stained gels (Fig. 4a, b). These results clearly suggest that the structural changes solely come from temperature.

3.3 Tau Conformation Monitored by Raman Spectroscopy

1. Raman spectra are recorded on a HR-800 Raman spectrophotometer equipped with achromatic Czerny-Turner type monochromator with silver treated mirrors and 800 mm focal length. The monochromatic radiation emitted by a He-Ne laser (633 nm), operating at 20 mW is used as a source. The instrument has Raman-shift detection accuracy of $\pm 1\text{ cm}^{-1}$ between 100 and 2000 cm^{-1} . The instrument is equipped with thermoelectrically cooled (with Peltier junctions), multi-channel, spectroscopic-grade charge coupled device (CCD) detec-

tor (1024×256 pixels of $26 \mu\text{m}$) with dark current lower than $0.002 \text{ electrons pixel}^{-1} \text{ s}^{-1}$ using a $50\times$ objective.

2. In order to record the temperature dependent Raman spectra using cooling-heating stage, the liquid protein samples are mounted on a LINKAM THMS 600 heating/freezing stage to which a temperature programmer TP 94 is connected with a temperature controller. Liquid nitrogen is used to maintain the stage at low temperature (*see* **Note 7**).
3. Temperature dependent Raman spectra of hTau40WT and hTau23WT protein samples are recorded at 10, 25, and 37°C . The Raman spectra are recorded only after incubating the sample at specific temperature for at least 5 min (*see* **Note 8**). All the parameters such as RTD exposure time = 15 s, exposure time = 15 s, accumulation number = 2, filter = D2, hole size = $400 \mu\text{m}$, slit = $100 \mu\text{m}$, grating = 1800 g/mm, are kept fixed while recording the Raman spectra for all the measurements.
4. The background correction and smoothening are performed for all the recorded spectra using instrumental software.
5. All the experiments are performed for at least two different occasions to check the reproducibility.

4 Notes

1. Tau is a soluble protein, which does not form any precipitates, but it aggregates if not handled properly.
2. Prior to the end of pelleting only supernatant is collected without touching the bottom of the tube, in order to not disturb the pellet, if any formed, otherwise the particles settled.
3. After purification and estimating the concentration, proper labeling is done and the protein samples are aliquoted and stored in -80°C as repeated freeze-thaw may lead to protein aggregation.
4. Centrifugation is done to remove the aggregated protein to ensure that only soluble protein is retained for sedimentation assay.
5. Incubation and pelleting are done at identical temperatures, i.e., if the protein is incubated at 10°C , it is pelleted at 10°C .
6. 1 mg/mL of hTau40WT and hTau23WT would correspond to 21.81 and $27.25 \mu\text{M}$, respectively.
7. The protein samples should be transferred carefully from the icebox to the Raman temperature stage so that the temperature of protein environment should not increase more than 10°C .

8. Raman measurements should start from 10 °C which would be beneficial for precise liquid state measurements and secondary structure prediction.

Acknowledgements

The authors thank Dr. Hirekodathakallu V. Thulasiram for his excellent Molecular Biology Laboratory (MBL) facility at the CSIR-NCL, Pune. Tau constructs were kindly gifted by Prof. Roland Brandt from University of Osnabruck, Germany and Prof. Jeff Kuret from Ohio State University College of Medicine, USA. Nalini Vijay Gorantla and Puneet Khandelwal acknowledge the fellowship from University Grant Commission and the Department of Biotechnology, India, respectively. This project is supported in part by grants from the DST-SERB (Young Investigator Grant): SB/YS/LS-355/2013, In-house NCL grant MLP029526 and CSIR-Network Project CSC0406. PP acknowledges support from CSIR-network project NANO-SHE. The authors have declared no conflict of interest.

References

1. Chen J, Kanai Y, Cowan NJ, Hirokawa N (1992) Projection domains of MAP2 and tau determine spacings between microtubules in dendrites and axons. *Nature* 360:674–677. doi:10.1038/360674a0
2. Butner KA, Kirschner MW (1991) Tau protein binds to microtubules through a flexible array of distributed weak sites. *J Cell Biol* 115:717–730
3. Kopke E, Tung YC, Shaikh S, Alonso AC, Iqbal K, Grundke-Iqbal I (1993) Microtubule-associated protein tau. Abnormal phosphorylation of a non-paired helical filament pool in Alzheimer disease. *J Biol Chem* 268: 24374–24384
4. Hirokawa N (1993) Axonal transport and the cytoskeleton. *Curr Opin Neurobiol* 3:724–731
5. Hirokawa N (1994) Microtubule organization and dynamics dependent on microtubule-associated proteins. *Curr Opin Cell Biol* 6:74–81
6. Hirokawa N, Shiomura Y, Okabe S (1988) Tau proteins: the molecular structure and mode of binding on microtubules. *J Cell Biol* 107:1449–1459
7. Hirokawa N, Takemura R (2005) Molecular motors and mechanisms of directional transport in neurons. *Nat Rev Neurosci* 6:201–214. doi:10.1038/nrn1624
8. Cleveland DW, Hwo SY, Kirschner MW (1977) Physical and chemical properties of purified tau factor and the role of tau in microtubule assembly. *J Mol Biol* 116:227–247
9. Garcia ML, Cleveland DW (2001) Going new places using an old MAP: tau, microtubules and human neurodegenerative disease. *Curr Opin Cell Biol* 13:41–48
10. Hoffman PN, Cleveland DW (1988) Neurofilament and tubulin expression recapitulates the developmental program during axonal regeneration: induction of a specific beta-tubulin isotype. *Proc Natl Acad Sci U S A* 85:4530–4533
11. Schweers O, Schönbrunn-Hanebeck E, Marx A, Mandelkow E (1994) Structural studies of tau protein and Alzheimer paired helical filaments show no evidence for beta-structure. *J Biol Chem* 269:24290–24297
12. Mandelkow E, Song YH, Schweers O, Marx A, Mandelkow EM (1995) On the structure of microtubules, tau, and paired helical filaments. *Neurobiol Aging* 16:347–354
13. Mandelkow EM, Schweers O, Drewes G, Biernat J, Gustke N, Trinczek B, Mandelkow E (1996) Structure, microtubule interactions, and phosphorylation of tau protein. *Ann N Y Acad Sci* 777:96–106
14. Schweers O, Mandelkow EM, Biernat J, Mandelkow E (1995) Oxidation of cysteine-322 in the repeat domain of microtubule-associated protein tau controls the in vitro

- assembly of paired helical filaments. *Proc Natl Acad Sci U S A* 92:8463–8467
15. von Bergen M, Barghorn S, Li L, Marx A, Biernat J, Mandelkow EM, Mandelkow E (2001) Mutations of tau protein in frontotemporal dementia promote aggregation of paired helical filaments by enhancing local beta-structure. *J Biol Chem* 276:48165–48174. doi:[10.1074/jbc.M105196200](https://doi.org/10.1074/jbc.M105196200)
16. Li L, von Bergen M, Mandelkow E-M, Mandelkow E (2002) Structure, stability, and aggregation of paired helical filaments from tau protein and FTDP-17 mutants probed by tryptophan scanning mutagenesis. *J Biol Chem* 277:41390–41400. doi:[10.1074/jbc.M206334200](https://doi.org/10.1074/jbc.M206334200)
17. Mylonas E, Hascher A, Bernadó P, Blackledge M, Mandelkow E, Svergun DI (2008) Domain conformation of tau protein studied by solution small-angle X-ray scattering. *Biochemistry* 47:10345–10353. doi:[10.1021/bi800900d](https://doi.org/10.1021/bi800900d)
18. Shkumatov AV, Chinnathambi S, Mandelkow E, Svergun DI (2011) Structural memory of natively unfolded tau protein detected by small-angle X-ray scattering. *Proteins* 79:2122–2131. doi:[10.1002/prot.23033](https://doi.org/10.1002/prot.23033)
19. Mandelkow E, von Bergen M, Biernat J, Mandelkow EM (2007) Structural principles of tau and the paired helical filaments of Alzheimer's disease. *Brain Pathol* 17:83–90. doi:[10.1111/j.1750-3639.2007.00053.x](https://doi.org/10.1111/j.1750-3639.2007.00053.x)
20. von Bergen M, Friedhoff P, Biernat J, Heberle J, Mandelkow EM, Mandelkow E (2000) Assembly of tau protein into Alzheimer paired helical filaments depends on a local sequence motif ((306)VQIVYK(311)) forming beta structure. *Proc Natl Acad Sci U S A* 97:5129–5134
21. Mukrasch MD, Biernat J, von Bergen M, Griesinger C, Mandelkow E, Zweckstetter M (2005) Sites of tau important for aggregation populate {beta}-structure and bind to microtubules and polyanions. *J Biol Chem* 280:24978–24986. doi:[10.1074/jbc.M501565200](https://doi.org/10.1074/jbc.M501565200)
22. von Bergen M, Barghorn S, Biernat J, Mandelkow EM, Mandelkow E (2005) Tau aggregation is driven by a transition from random coil to beta sheet structure. *Biochim Biophys Acta* 1739:158–166. doi:[10.1016/j.bbadis.2004.09.010](https://doi.org/10.1016/j.bbadis.2004.09.010)
23. von Bergen M, Barghorn S, Jeganathan S, Mandelkow EM, Mandelkow E (2006) Spectroscopic approaches to the conformation of tau protein in solution and in paired helical filaments. *Neurodegener Dis* 3:197–206. doi:[10.1159/000095257](https://doi.org/10.1159/000095257)
24. von Bergen M, Barghorn S, Muller SA, Pickhardt M, Biernat J, Mandelkow EM, Davies P, Aebl U, Mandelkow E (2006) The core of tau-paired helical filaments studied by scanning transmission electron microscopy and limited proteolysis. *Biochemistry* 45:6446–6457. doi:[10.1021/bi052530j](https://doi.org/10.1021/bi052530j)
25. Mukrasch MD, Bibow S, Korukottu J, Jeganathan S, Biernat J, Griesinger C, Mandelkow E, Zweckstetter M (2009) Structural polymorphism of 441-residue tau at single residue resolution. *PLoS Biol* 7:e34. doi:[10.1371/journal.pbio.1000034](https://doi.org/10.1371/journal.pbio.1000034)
26. Lippens G, Sillen A, Smet C, Wieruszski JM, Leroy A, Buee L, Landrieu I (2006) Studying the natively unfolded neuronal Tau protein by solution NMR spectroscopy. *Protein Pept Lett* 13:235–246. doi:[10.2174/092986606775338461](https://doi.org/10.2174/092986606775338461)
27. Sibille N, Sillen A, Leroy A, Wieruszski JM, Mulloy B, Landrieu I, Lippens G (2006) Structural impact of heparin binding to full-length Tau as studied by NMR spectroscopy. *Biochemistry* 45:12560–12572. doi:[10.1021/bi060964o](https://doi.org/10.1021/bi060964o)
28. Zingsheim HP, Herzog W, Weber K (1979) Differences in surface morphology of microtubules reconstituted from pure brain tubulin using two different microtubule-associated proteins: the high molecular weight MAP 2 proteins and tau proteins. *Eur J Cell Biol* 19:175–183
29. Wille H, Drewes G, Biernat J, Mandelkow EM, Mandelkow E (1992) Alzheimer-like paired helical filaments and antiparallel dimers formed from microtubule-associated protein tau in vitro. *J Cell Biol* 118:573–584
30. Jeganathan S, Chinnathambi S, Mandelkow E-M, Mandelkow E (2012) Conformations of microtubule-associated protein Tau mapped by fluorescence resonance energy transfer. *Methods Mol Biol* 849:85–99. doi:[10.1007/978-1-61779-551-0_7](https://doi.org/10.1007/978-1-61779-551-0_7)
31. Jeganathan S, von Bergen M, Brutlach H, Steinhoff HJ, Mandelkow E (2006) Global hairpin folding of tau in solution. *Biochemistry* 45:2283–2293. doi:[10.1021/bi0521543](https://doi.org/10.1021/bi0521543)
32. Siddiqua A, Margittai M (2010) Three- and four-repeat Tau coassemble into heterogeneous filaments: an implication for Alzheimer disease. *J Biol Chem* 285:37920–37926. doi:[10.1074/jbc.M110.185728](https://doi.org/10.1074/jbc.M110.185728)
33. Becker JS, Przybylski M (2007) Studies of structure and phosphorylation of tau protein using high resolution mass spectrometry. *J Anal At Spectrom* 22:761. doi:[10.1039/b701440f](https://doi.org/10.1039/b701440f)

34. Schwalbe M, Ozenne V, Bibow S, Jaremko M, Jaremko L, Gajda M, Jensen MR, Biernat J, Becker S, Mandelkow E, Zweckstetter M, Blackledge M (2014) Predictive atomic resolution descriptions of intrinsically disordered hTau40 and α -synuclein in solution from NMR and small angle scattering. *Structure* 22:238–249. doi:[10.1016/j.str.2013.10.020](https://doi.org/10.1016/j.str.2013.10.020)
35. Bernadó P, Svergun DI (2012) Analysis of intrinsically disordered proteins by small-angle X-ray scattering. *Methods Mol Biol* 896:107–122. doi:[10.1007/978-1-4614-3704-8_7](https://doi.org/10.1007/978-1-4614-3704-8_7)
36. Jeganathan S, Hascher A, Chinnathambi S, Biernat J, Mandelkow EM, Mandelkow E (2008) Proline-directed pseudo-phosphorylation at AT8 and PHF1 epitopes induces a compaction of the paperclip folding of Tau and generates a pathological (MC-1) conformation. *J Biol Chem* 283:32066–32076. doi:[10.1074/jbc.M805300200](https://doi.org/10.1074/jbc.M805300200)
37. von Bergen M, Li L, Mandelkow E (2005) Intrinsic fluorescent detection of tau conformation and aggregation. *Methods Mol Biol* 299:175–184
38. Herrero AM, Cambero MI, Ordóñez JA, de la Hoz L, Carmona P (2008) Raman spectroscopy study of the structural effect of microbial transglutaminase on meat systems and its relationship with textural characteristics. *Food Chem* 109:25–32. doi:[10.1016/j.foodchem.2007.12.003](https://doi.org/10.1016/j.foodchem.2007.12.003)
39. McColl IH, Blanch EW, Gill AC, Rhie AGO, Ritchie MA, Hecht L, Nielsen K, Barron LD (2003) A new perspective on beta-sheet structures using vibrational Raman optical activity: from poly(L-lysine) to the prion protein. *J Am Chem Soc* 125:10019–10026. doi:[10.1021/ja021464v](https://doi.org/10.1021/ja021464v)
40. Arya S, Kumari A, Dalal V, Bhattacharya M, Mukhopadhyay S (2015) Appearance of annular ring-like intermediates during amyloid fibril formation from human serum albumin. *Phys Chem Chem Phys* 17:22862–22871. doi:[10.1039/C5CP03782D](https://doi.org/10.1039/C5CP03782D)
41. Kurouski D, Lu X, Popova L, Wan W, Shanmugasundaram M, Stubbs G, Dukor RK, Lednev IK, Nafie LA (2014) Is supramolecular filament chirality the underlying cause of major morphology differences in amyloid fibrils? *J Am Chem Soc* 136:2302–2312. doi:[10.1021/ja407583r](https://doi.org/10.1021/ja407583r)
42. Zhu F, Davies P, Thompson AR, Kelly SM, Tranter GE, Hecht L, Isaacs NW, Brown DR, Barron LD (2008) Raman optical activity and circular dichroism reveal dramatic differences in the influence of divalent copper and manganese ions on prion protein folding. *Biochemistry* 47:2510–2517. doi:[10.1021/bi7022893](https://doi.org/10.1021/bi7022893)
43. Silva JG, Arruda LM, Pinheiro GS, Lima CL, Melo FEA, Ayala AP, Filho JM, Freire PTC (2015) The temperature-dependent single-crystal Raman spectroscopy of a model dipeptide: L-Alanyl-L-alanine. *Spectrochim Acta A Mol Biomol Spectrosc* 148:244–249. doi:[10.1016/j.saa.2015.04.010](https://doi.org/10.1016/j.saa.2015.04.010)
44. Accardo A, Shalabaeva V, Cotte M, Burghammer M, Krahne R, Riekel C, Dante S (2014) Amyloid β peptide conformational changes in the presence of a lipid membrane system. *Langmuir* 30:3191–3198. doi:[10.1021/la500145r](https://doi.org/10.1021/la500145r)
45. Ramachandran G, Milán-Garcés EA, Udgaonkar JB, Puranik M (2014) Resonance Raman spectroscopic measurements delineate the structural changes that occur during tau fibril formation. *Biochemistry* 53:6550–6565. doi:[10.1021/bi500528x](https://doi.org/10.1021/bi500528x)
46. Maiti NC, Apetri MM, Zagorski MG, Carey PR, Anderson VE (2004) Raman spectroscopic characterization of secondary structure in natively unfolded proteins: alpha-synuclein. *J Am Chem Soc* 126:2399–2408. doi:[10.1021/ja0356176](https://doi.org/10.1021/ja0356176)
47. Ishizaki H, Balaram P, Nagaraj R, Venkatachalapathi YV, Tu AT (1981) Determination of beta-turn conformation by laser Raman spectroscopy. *Biophys J* 36:509–517. doi:[10.1016/S0006-3495\(81\)84749-2](https://doi.org/10.1016/S0006-3495(81)84749-2)
48. Barghorn S, Biernat J, Mandelkow E (2005) Purification of recombinant tau protein and preparation of Alzheimer-paired helical filaments in vitro. *Methods Mol Biol* 299:35–51

Tau Protein

Methods and Protocols

Smet-Nocca, C. (Ed.)

2017, XVIII, 432 p. 83 illus., 64 illus. in color., Hardcover

ISBN: 978-1-4939-6596-0

A product of Humana Press